Characterization of Full Length and Truncated Type I Human Methionine Aminopeptidases Expressed from *Escherichia coli*†

Jing-Ya Li,‡ Ling-Ling Chen,‡ Yong-Mei Cui,‡ Qun-Li Luo,‡ Min Gu,‡ Fa-Jun Nan,*,‡ and Qi-Zhuang Ye*,‡,§

Chinese National Center for Drug Screening, Shanghai Institute of Materia Medica, Shanghai Institutes for Biological Sciences, Chinese Academy of Sciences, Shanghai 201203, China, and The High Throughput Screening Laboratory, Higuchi Biosciences Center, University of Kansas, Lawrence, Kansas 66047

Received November 20, 2003; Revised Manuscript Received March 5, 2004

ABSTRACT: Methionine aminopeptidase (MetAP) carries out an essential posttranslational modification of nascent proteins by removing the initiator methionine and is recognized as a potential target for developing antibacterial, antifungal, and anticancer agents. We have established an *Escherichia coli* expression system for human type I MetAP (*Hs*MetAP1) and characterized the full length *Hs*MetAP1 and its N-terminal-truncated mutants *Hs*MetAP1(Δ1−66) and *Hs*MetAP1(Δ1−135) for hydrolysis of several thiopeptolide and peptide substrates and inhibition by a series of nonpeptidic inhibitors. Although the N-terminal extension with zinc finger motifs in *Hs*MetAP1 is not required for enzyme activity, it has a significant impact on the interaction of the enzyme with substrates and inhibitors. In hydrolysis of the thiopeptolide substrates, a relaxation of stringent specificity for the terminal methionine was observed in the truncated mutants. However, this relaxation of specificity was not detectable in hydrolysis of tripeptide or tetrapeptide substrates. Several nonpeptidic inhibitors showed potent inhibition of the mutant *Hs*MetAP1(Δ1−66) but exhibited only weak or no inhibition of the full length enzyme. With the recombinant *Hs*MetAP1 available, we have identified several MetAP inhibitors with submicromolar inhibitory potencies against *E. coli* MetAP (*Ec*MetAP1) that do not affect *Hs*MetAP1. These results have demonstrated the possibility of developing MetAP inhibitors as antibacterial agents with minimum human toxicity. In addition, micromolar inhibitors of *Hs*MetAP1 identified in this study can serve as tools for investigating the functions of *Hs*MetAP1 in physiological and pathological processes.

Protein biosynthesis is initiated with either Met (in eukaryotes) or *N*-formylmethionine (in prokaryotes, mitochondria, and chloroplasts) (*1*). In a significant fraction of intracellular proteins, the N-terminal Met is cleaved enzymatically after the initiation of translation by methionine aminopeptidase (MetAP).[1] This posttranslational modification is often required for proper localization, targeting, and eventual degradation of proteins.

MetAP maintains stringent specificity for the N-terminal Met (*2*) and accepts no other natural amino acid residues. The formyl group in formylmethionine must be removed by deformylase before Met can be cleaved by MetAP (*3*). The enzyme also has a strong preference for the penultimate residue, and only a small, uncharged amino acid (Gly, Ala, Ser, Thr, Pro, Val, or Cys) allows MetAPs to cleave the N-terminal Met.

MetAPs are grouped into two subtypes according to sequence homology. Eubacteria, such as *Escherichia coli*, *Bacillus subtilis*, and *Salmonella typhimurium*, have only type I MetAPs, while archaea, such as *Methanobacterium thermoautotrophicum*, *Sulfolobus solfataricus*, and *Pyrococcus furiosis*, have only type II MetAPs. Eukaryotic cells contain both type I and type II MetAPs (*1*). The most significant difference between these two types is an insertion of approximately 60 residues in the C-terminal aminopeptidase domain characteristic of the type II isozymes (*4*). This inserted subdomain shares no sequence or structural homology with any other known protein, and its function is unknown.

The eukaryotic MetAPs are differentiated from their prokaryotic counterparts by an additional N-terminal extension. The eukaryotic type I MetAPs have two putative zinc finger motifs in this 12 kDa region (*5*), and the eukaryotic type II enzymes have a highly charged N-terminus with alternating polyacidic and polybasic stretches in a similarly sized segment (*6*). These N-terminal extensions may be involved in the association of eukaryotic MetAP isozymes with intracellular structures or organelles such as the ribosome (*7*).

† This research was supported by the National Natural Science Foundation of China Grants 30271528 (F.-J.N.) and 39725032 (Q.-Z.Y.) and by the NIH Grant P20 RR15563 from the COBRE Program of the National Center for Research Resources and matching support from the State of Kansas and the University of Kansas (Q.-Z.Y.).

* To whom correspondence should be addressed. (Q.-Z.Y.) Phone: (785)330-4330. Fax: (785)330-4332. E-mail: qye@ku.edu. (F.-J.N.) Phone: 86-21-5080-1313. Fax: 86-21-5080-0721. E-mail: fjnan@mail.shcnc.ac.cn.

‡ Chinese National Center for Drug Screening.

§ University of Kansas.

[1] Abbreviations: MetAP, methionine aminopeptidase; *Ec*MetAP1, *E. coli* MetAP type I; *Hs*MetAP1, human MetAP type I; GST, glutathione S-transferase; DTNB, 5,5-dithiobis(2-nitrobenzoic acid); Nle, norleucine.

10.1021/bi0360859 CCC: $27.50
Published on Web 05/07/2004

Deletion of the single MetAP gene from *E. coli* (*8*) or *S. typhimurium* (*9*) is lethal, demonstrating the essential role of MetAP enzymes in bacteria. Deletion of either type I or type II MetAP from the yeast *Saccharomyces cerevisiae* rendered a slow growth phenotype, and removal of both MetAPs made the yeast nonviable (*10*). Therefore, MetAPs are valid potential targets for developing antibacterial and antifungal drugs (*11*).

The enterohemorrhagic *E. coli* O157:H7 strain and the common K-12 strain have the same MetAP sequence (*12*). The *E. coli* MetAP, a type I enzyme (*Ec*MetAP1), shares high sequence homology with MetAPs in other clinically important pathogens such as *Mycobacterium tuberculosis* in tuberculosis, *Enterococcus faecalis* in urinary tract infection and endocarditis, *Streptococcus pneumoniae* in pneumonia, *Haemophilus influenzae* in respiratory tract infection, and *Helicobacter pylori* in ulcers. MetAPs in these pathogens are all type I enzymes, and the sequence homology among them provides a convenient way to translate knowledge from *Ec*MetAP1 to other type I MetAPs. However, the sequence similarity in type I MetAPs also presents a challenge in developing specific inhibitors for bacterial and fungal MetAP1s without affecting human type I enzyme (*Hs*-MetAP1).

We report here a unique *E. coli* expression system for the full length *Hs*MetAP1, as well as for N-terminal-truncated *Hs*MetAP1 mutants. These proteins have been characterized for catalysis and inhibition with several peptide and thiopeptolide substrates and nonpeptidic inhibitors. We have observed a significant influence of the N-terminal extension on catalysis and inhibition and also identified inhibitors with specificity for *Ec*MetAP1 and potent inhibitors of *Hs*MetAP1. These studies provide valuable information for developing MetAP inhibitors for therapeutic applications.

EXPERIMENTAL PROCEDURES

Materials and Instruments. The plasmid pGEX-KG (*13*) was a generous gift from Professor Kunliang Guan at the University of Michigan, and the *E. coli* strain BL21(DE3)-pLysS was purchased from Promega (Madison, WI). Restriction enzymes and other enzymes used in DNA cloning were purchased from Sangon (Shanghai, China). Thrombin and Ellman's reagent DTNB was purchased from Sigma (St. Louis, MO). Thioester substrate Met-S-Gly-Phe was synthesized in this laboratory according to a literature procedure (*14*). Synthesis of the nonpeptidic inhibitors has been reported previously (*15*), and synthesis of the thiopeptolides Xaa-S-Gly-Phe will be reported elsewhere. Tripeptide substrates Xaa-Ala-Ser, where Xaa is norleucine (Nle), Leu, or Phe, and tetrapeptide substrates Xaa-Ala-Ser-Trp, where Xaa is Ile, Leu, Met, Phe, Thr, or Val, were synthesized by GL Biochem (Shanghai, China). Met-Ala-Ser was purchased from Sigma.

Protein purification was carried out on an AKTA FPLC system with UV and conductivity monitors from Amersham Biosciences (Piscataway, NJ), and the protein concentration was determined by the BCA protein assay with a kit from PIERCE (Rockford, IL). Enzyme assays were performed on a SpectraMax 340 microplate reader from Molecular Devices (Sunnyvale, CA) that was controlled by Softmax software.

Construction of Plasmids Expressing Full Length and Truncated HsMetAP1s. A cDNA library was prepared by reverse transcription PCR amplification from total RNA of ECV304 cultured bladder carcinoma cells (ATCC CRL-1998). The full length gene of *Hs*MetAP1 was amplified from the cDNA library with introduction of restriction sites for *Eco*R I and *Sal* I. The PCR primers had the following sequence: forward, ATTATAA*GAATTC*TAATGGCGGC-CGTGGAGAC GCGG, and reverse, ACGGTA*GTCGAC*-TTAAAATTGAGACATGAAG TG (the restriction sites are in italics, and the coding sequences are underlined). The PCR fragment was cloned into the vector pGEX-KG (*13*) as a fusion protein with an N-terminal glutathione S-transferase (GST). The recombinant plasmid, pGEX-KG/*Hs*MetAP1, was confirmed by DNA sequencing and transformed into *E. coli* strain BL21(DE3)pLysS for expression.

The genes for the truncated mutants *Hs*MetAP1-(Δ1−66) and *Hs*MetAP1(Δ1−135) were amplified by PCR from pGEX-KG/*Hs*MetAP1 using forward primers TAGG*GAATTC*TATGGACTGTGGAAGGTGATATT and ATCA*GAATTC*TAATAGAAGGGATGCGACTTGTA, respectively. The PCR fragments were also cloned into the vector pGEX-KG for expression.

Expression and Purification of Full Length and Truncated HsMetAP1s. E. coli cells containing the plasmid pGEX-KG/*Hs*MetAP1 were cultured in 1 L of LB medium at 37 °C. Expression of the recombinant GST-*Hs*MetAP1 protein was induced at an OD of 0.6 by adding IPTG to 0.5 mM and allowed to continue for 5 h at 30 °C. Harvested cells (2.0 g) were resuspended in 200 mL of PBS buffer (140 mM NaCl, 2.7 mM KCl, 10 mM Na_2HPO_4, and 1.8 mM KH_2PO_4) with 1% Triton X-100 and sonicated for 5 min on ice. After centrifugation at 12 000*g* for 15 min, the clarified supernatant was loaded onto a 5 mL GSTrap FF column previously equilibrated with the PBS buffer, and the GST-*Hs*MetAP1 fusion protein was eluted with 10 mM reduced glutathione in 50 mM Tris, pH 8.0. Then, the eluted fractions were loaded onto a 55 mL HiPrep desalting column pre-equilibrated with 50 mM Tris, pH 8.0, and 150 mM NaCl to remove the reduced glutathione. Active *Hs*MetAP1 was released from the fusion protein by incubation with 2 μg/mL thrombin and 1.5 mM $CaCl_2$ at 4 °C overnight, and the mixture was loaded on the GSTrap FF column to remove the GST protein. The final *Hs*MetAP1 protein (10 mg) appeared as a single band on SDS-PAGE gel by Coomassie blue staining.

Similarly, the truncated *Hs*MetAP1(Δ1−66) and *Hs*-MetAP1(Δ1−135) were expressed at 30 °C for 5 h and at 16 °C for 18 h, respectively, after induction by IPTG and purified to homogeneity.

Enzyme Activity Assays. Thiopeptolide Assay. The assay was performed at room temperature on a 96 well clear polystyrene microplate. In the metal activation experiments, the assay mixture in each well contained 50 mM MOPS, pH 7.0, 1 mM 5,5′-dithiobis(2-nitrobenzoic acid) (DTNB), 100 μM Met-S-Gly-Phe, 750 nM *Hs*MetAP1 or 650 nM *Hs*MetAP1(Δ1−66), and various amounts of metal ions ($CoCl_2$, $MnCl_2$, $ZnCl_2$, or $NiCl_2$). The hydrolysis of Met-S-Gly-Phe was monitored continuously by the change of absorbance at 412 nm. The initial rate of the hydrolysis was determined using the early linear portion of the enzymatic reaction curve, and the rate of background hydrolysis of the

thiopeptolide was subtracted.

To obtain the k_{cat} and K_m values using Met-S-Gly-Phe, the reaction was carried out in a 100 μL assay mixture containing 50 mM MOPS, pH 7.0, 50 μM $CoCl_2$, 500−750 nM *Hs*MetAP1s, and thiopeptolide Met-S-Gly-Phe in 2-fold dilutions up to 10 mM for 2 min at room temperature. A 50 μL solution containing 2 mM DTNB, 50 mM MOPS, pH 7.0, and 6 M guanidine hydrochloride was added to the mixture, and the absorbance at 412 nm was determined immediately. The rate of background hydrolysis of the thiopeptolide was subtracted. The k_{cat} and K_m values of *Hs*MetAP1s were derived from a nonlinear regression fitting of the curve in the plot of the initial rates vs the substrate concentrations, using the Michaelis−Menton equation $v = V_{max}[S]/(K_m + [S])$. In the inhibition assays, the inhibitor was dissolved in DMSO, and the final assay system had less than 2% DMSO.

For hydrolysis of thiopeptolide substrates Xaa-S-Gly-Phe, the reaction was carried out in a 100 μL assay mixture containing 50 mM MOPS, pH 7.0, 50 μM $CoCl_2$, 200 nM *Ec*MetAP1 or 500−750 nM *Hs*MetAP1, *Hs*MetAP1(Δ1−66) or *Hs*MetAP1(Δ1−135), 500 μM Xaa-S-Gly-Phe, and 1 mM DTNB. Change in the absorbance at 412 nm was monitored continuously for 1 min at room temperature.

Peptide Assay. Assays with tripeptide substrates Xaa-Ala-Ser were performed at room temperature in a 20 μL reaction system containing 50 mM MOPS, pH 7.0, 50 μM $CoCl_2$, 8 mM Xaa-Ala-Ser, and 5 μM *Ec*MetAP1 for 5 min or 1 μM *Hs*MetAP1, *Hs*MetAP1(Δ1−66), or *Hs*MetAP1(Δ1−135) for 30 min. The reaction was terminated by adding 80 μL of 0.1% trifluoroacetic acid (TFA), and the mixture was applied to a reverse-phase HPLC C8 column (4.6 × 150 mm, 5 μm) after centrifugation at 10 000*g* for 10 min. The elution conditions were as follows: mobile phase A was water with 0.1% TFA, and mobile phase B was 50% acetonitrile with 0.1% TFA; the sample was loaded onto the column by 5% phase B at a flow rate of 1 mL/min. Then, 100% phase B was used to elute any residual material in 15 min before returning to the initial conditions. The product released was calculated from substrate depletion, which was determined by monitoring the absorbance at 215 nm.

Assays with tetrapeptide substrates Xaa-Ala-Ser-Trp were performed in a similar way. Xaa-Ala-Ser-Trp (5 mM) and 1 μM *Ec*MetAP1, *Hs*MetAP1, *Hs*MetAP1(Δ1−66), or *Hs*MetAP1(Δ1−135) were used, and the reaction was terminated after 5 min. The sample was loaded onto a C18 column (4.6 × 150 mm, 5 μm) by 40% phase B at a flow rate of 1 mL/min. The product Ala-Ser-Trp released from the reaction was monitored by absorbance at 215 nm and used for calculations.

RESULTS

E. coli Expression of Full Length HsMetAP1. Recombinant expression and purification of *Hs*MetAP1 has been reported only briefly in insect cells (*16*). Dummitt et al. (*17*) described the expression of *Hs*MetAP1 in *S. cerevisiae* for an in vivo study without purification. To facilitate our mutagenesis studies and generate a sufficient amount of recombinant proteins for enzyme characterization, our laboratory has successfully established the first *Hs*MetAP1 expression system in *E. coli*.

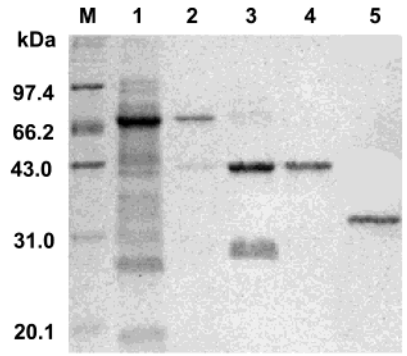

FIGURE 1: Purification of *Hs*MetAP1. Lane M, protein markers; lane 1, cell lysate containing GST-*Hs*MetAP1; lane 2, purified GST-*Hs*MetAP1; lane 3, after thrombin cleavage; lane 4, purified *Hs*MetAP1; lane 5, N-terminal-truncated *Hs*MetAP1.

An expression plasmid was constructed so that *Hs*MetAP1 was expressed as a fusion protein with an N-terminal glutathione S-transferase (GST) and a thrombin cleavage site was located between the GST and *Hs*MetAP1. The recombinant GST-*Hs*MetAP1 fusion protein was expressed in *E. coli* as a soluble protein after IPTG induction and purified on a glutathione−Sepharose affinity column (Figure 1). Thrombin treatment released *Hs*MetAP1 from the fusion protein, and the yield after thrombin cleavage was usually 5−10 mg from a 1 L culture. Molecular mass measured by matrix-assisted laser desorption ionization time-of-flight (MALDI-TOF) for the released *Hs*MetAP1 was 44 199 Da, consistent with the calculated value from the amino acid sequence, 44 207 Da.

Specific N-Terminal Truncation of Full Length HsMetAP1. The recombinant *Hs*MetAP1 was not very stable during purification and storage at 4 °C, and a smaller but enzymatically active protein appeared at around 36 kDa. We purified the 36 kDa fragment (Figure 1, lane 5) and performed N-terminal sequencing. The sequence, WTVEGD, suggested a hydrolytic site located between Ser-66 and Trp-67 of the N-terminus of *Hs*MetAP1 following the predicted zinc finger motifs (Figure 2). This truncated enzyme cleaved the synthetic substrates (peptides and thiopeptolides) as efficiently as the full length enzyme, indicating that the N-terminal extension was not indispensable for *Hs*MetAP1 aminopeptidase activity. Our observation is consistent with the reports that the N-terminal extension in eukaryotic MetAPs (Figure 2) can be truncated without losing peptidase activity in *S. cerevisiae* type I methionine aminopeptidase (*Sc*MetAP1) (*5*) and human type II methionine aminopeptidase (*Hs*MetAP2) (*18*).

On the basis of the finding that the N-terminal truncation of *Hs*MetAP1 retains enzymatic activity, we constructed two truncated mutants to study the role of the N-terminal extension in catalysis and inhibition. Mutant *Hs*MetAP1-(Δ1−66) began at Trp-67 with the zinc finger motifs removed, and mutant *Hs*MetAP1(Δ1−135) began at Ile-136 with complete removal of the N-terminal extension found in eukaryotic type I MetAPs. Both were expressed as GST fusion proteins and purified similarly as the full length *Hs*MetAP1.

Hydrolysis of the Thiopeptolide Substrate Met-S-Gly-Phe by Full Length and Truncated HsMetAP1s. MetAPs have been studied as Co(II) enzymes, but their in vivo

```
                                                                10        20        30        40        50        60
HsMetAP1                                                        MAAVETRVCETDGCSSEAKLQCPTCIKLGIQGSYFCSQECFKGSWATHKLLHKKAKDEKA
HsMetAP2                MAGVEEVAASGSHLNGDLDPDDREEGAASTAEEAAKKKRRKKKKSKGPSAAGEQEPDKESGASVDEVARQLERSALEDKERDEDDEDGDG
ScMetAP1                                                        MSTATTTVTTSDQASHPTKIYCSGLQCGRETSSQMKCPVCLKQGIVSIFCDTSCYENNY

                    70        80        90        100       110       120       130       140       150       160
HsMetAP1        KREVSSWTVEGDINTDPWAGYRYTGKLRPHYPLMPTRPVPSYIQRPDYADHPLGMSESEQALKGTSQIKLLSSEDIEGMRLVCRLAREVLDVAAGMIKPG
HsMetAP2        DGDGATGKKKKKKKKKRGPKVQTDPPSVPICDLYPNGVFPKGQECEYPPTQDGRTAAWRTTSEEKKALDQASEEIWNDFREAAEAHRQVRKYVMSWIKPG
ScMetAP1        KAHKALHNAKDGLEGAYDPFPKFKYSGKVKASYPLTPRRYVPEDIPKPDWAANGLPVSEQRNDRLNNIPIYKKDQIKKIRKACMLGREVLDIAAAHVRPG
EcMetAP1                                                                                MAISIKTPEDIEKMRVAGRLAAEVLEMIEPYVKPG
```

FIGURE 2: N-Terminal sequence comparison among MetAPs from human (type I, *Hs*MetAP1 and type II, *Hs*MetAP2), *S. cerevisiae* (type I, *Sc*MetAP1), and *E. coli* (type I, *Ec*MetAP1). Truncations in *Hs*MetAP2 reported by Yang et al. (*18*), in *Sc*MetAP1 reported by Zou et al. (*5*), and in *Hs*MetAP1 described here are underlined. Putative zinc finger residues are shown in bold face.

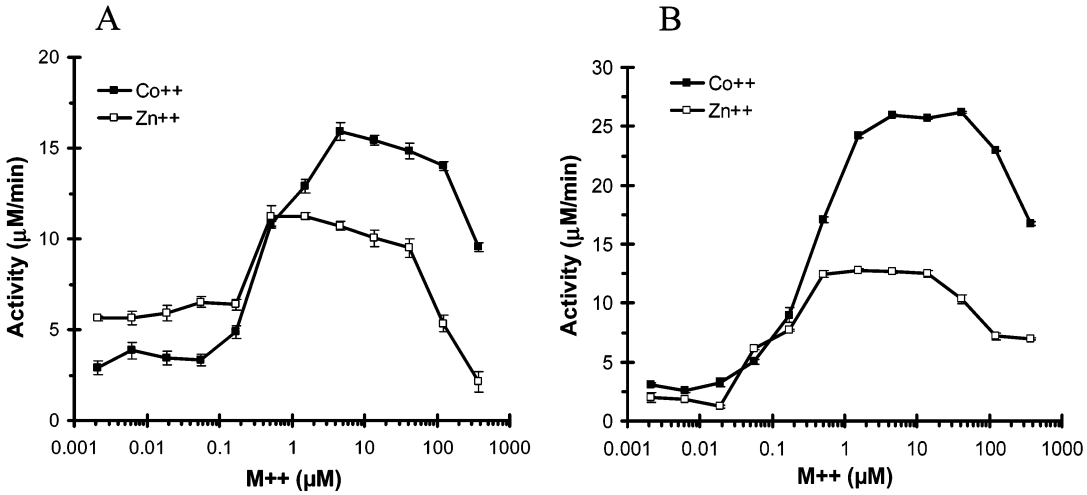

FIGURE 3: Activation of full length *Hs*MetAP1 (A) and truncated mutant *Hs*MetAP1(Δ1−66) (B) by divalent ions Co(II) (filled squares) and Zn(II) (open squares). The metal activation assay was carried out in a 100 μL mixture including 50 mM MOPS, pH 7.0, 750 nM *Hs*MetAP1 or 650 nM *Hs*MetAP1(Δ1−66), 100 μM Met-S-Gly-Phe, and one of the divalent ions.

metal remains to be defined. A few other divalent metals are also capable of activating the enzyme in vitro (*19*, *20*). Using thiopeptolide Met-S-Gly-Phe as the substrate, both the full length *Hs*MetAP1 and the truncated mutant *Hs*MetAP1(Δ1−66) can be activated by Co(II) and Zn(II) (Figure 3). However, neither Ni(II) nor Mn(II) can activate the full length enzyme or the truncated mutant *Hs*MetAP1-(Δ1−66). *Hs*MetAP1(Δ1−135) can also be activated by Co(II), but its activity was much weaker. Meanwhile, excess Co(II) and Zn(II) appeared to have an inhibitory effect on the intact and truncated *Hs*MetAP1s (Figure 3).

The truncated *Sc*MetAP1 had essentially the same K_m and k_{cat} values as the full length enzyme (*5*). The intact and truncated *Hs*MetAP2 enzymes exhibited identical kinetic behavior and physical properties (*18*). In this study, two forms of truncated *Hs*MetAP1s were prepared and kinetic properties were investigated along with the full length enzyme. To avoid DTNB inactivation in the thiopeptolide assay, an endpoint method was employed. *Hs*MetAP1(Δ1−66) was found to cleave the substrate Met-S-Gly-Phe more efficiently with slightly lower K_m and higher k_{cat} values (Table 1). At the same time, more extensive deletion of the N-terminus as in *Hs*MetAP1(Δ1−135) resulted in much lower activity, mostly as a higher K_m. These results suggest that the N-terminal extension in *Hs*MetAP1 is not essential for catalytic activity, but its existence does affect the catalytic efficiency in hydrolyzing the thiopeptolide as indicated by altered K_{cat} and K_m values for the truncated mutants.

Hydrolysis of Thiopeptolide Substrates Xaa-S-Gly-Phe and Peptide Substrates Xaa-Ala-Ser by Full Length and Truncated HsMetAP1s. To determine the effect of these truncations on the specificity toward substrates and inhibitors, several specially synthesized substrates (thiopeptolides Xaa-S-Gly-Phe and peptides Xaa-Ala-Ser and Xaa-Ala-Ser-Trp) and a series of nonpeptidic inhibitors (*15*) were used.

Table 1: Kinetic Constants of *Ec*MetAP1 and Full Length and Truncated *Hs*MetAP1s in Hydrolysis of the Thiopeptolide Met-S-Gly-Phe

	K_m (mM)	k_{cat} (s^{-1})	k_{cat}/K_m (M^{-1} s^{-1})
*Ec*MetAP1	0.35 ± 0.01	22.48 ± 0.32	63 835
*Hs*MetAP1	1.88 ± 0.02	6.47 ± 0.47	3451
*Hs*MetAP1(Δ1−66)	1.28 ± 0.04	16.61 ± 1.13	12 956
*Hs*MetAP1(Δ1−135)	8.81 ± 0.44	7.31 ± 0.18	829

MetAP is very specific for Met as the terminal residue, as exemplified by *Ec*MetAP1 in cleavage of Xaa-S-Gly-Phe (Table 2). Full length *Hs*MetAP1 maintains specificity for Met, and only Thr showed weakly detectable activity. Surprisingly, *Hs*MetAP1(Δ1−66) cleaved the thiopeptolide with Leu, Phe, Val, or Thr, in addition to Met, as the starting residue (Table 2). This specificity is further relaxed in the mutant *Hs*MetAP1(Δ1−135). Hydrolysis was detected in several such thiopeptolides, and some residues such as Phe and Val even became the preferred residue over Met.

Considering the heightened reactivity intrinsic to Xaa-S-Gly-Phe substrates, parallel assays were carried out using substrates with true peptide bonds. The tripeptides Xaa-Ala-Ser were incubated with *Ec*MetAP1, full length *Hs*MetAP1, and its mutants *Hs*MetAP1(Δ1−66) and *Hs*MetAP1(Δ1−135) for a period of time. The products were separated from the unreacted starting substrate by HPLC. Met-Ala-Ser and Nle-

Table 2: Substrate Specificity of Full Length and Truncated *Hs*MetAP1s in Comparison with *Ec*MetAP1

Xaa residue	activity (μM/min/μM protein) *Ec*Met-AP1	*Hs*Met-AP1	*Hs*Met-AP1(Δ1−66)	*Hs*Met-AP1(Δ1−135)
Thiopeptolide Substrate Xaa-S-Gly-Phe				
Met	362 ± 24	42.7 ± 5.8	146 ± 9	18.4 ± 1.3
Ala	NA[a]	NA	NA	9.4 ± 2.5
Asp	NA	NA	NA	NA
Ile	NA	NA	NA	NA
Leu	NA	NA	5.4 ± 0.3	13.4 ± 1.6
Lys	NA	NA	NA	16.0 ± 1.5
Phe	NA	NA	7.4 ± 0.8	25.5 ± 1.4
Pro	NA	NA	NA	15.2 ± 0.3
Ser	NA	NA	NA	11.7 ± 1.2
Tyr	NA	NA	NA	15.0 ± 0.3
Val	NA	NA	8.1 ± 1.0	30.4 ± 2.3
Gly	NA	NA	NA	NA
Thr	NA	7.3 ± 1.3	12.1 ± 0.2	8.8 ± 1.1
Asn	NA	NA	NA	6.0 ± 2.1
Trp	NA	NA	NA	NA
Tripeptide Substrate Xaa-Ala-Ser				
Met	248 ± 9	142 ± 13	100 ± 13	NA
Nle	279 ± 4	183 ± 12	141 ± 10	1.3 ± 0.7
Leu	NA	NA	NA	NA
Phe	NA	NA	NA	NA
Tetrapeptide Substrate Xaa-Ala-Ser-Trp				
Met	212 ± 15	396 ± 20	201 ± 15	NA
Leu	3.5 ± 1.0	30 ± 2	23 ± 0.2	NA
Phe	16 ± 0.2	30 ± 4	22 ± 3	NA
Ile	NA	NA	NA	NA
Val	NA	NA	NA	NA
Thr	NA	NA	NA	NA

[a] NA, no activity was detected (<5.0 for the thiopeptolide assays or <1.0 for the peptide assays).

Ala-Ser were good substrates for *Ec*MetAP1, *Hs*MetAP1, and *Hs*MetAP1(Δ1−66), while the other two tripeptides Leu-Ala-Ser and Phe-Ala-Ser showed no cleavage. *Hs*MetAP1-(Δ1−135) is a much less efficient enzyme for the peptides tested, and only Nle-Ala-Ser showed barely detectable cleavage.

Walker et al. (*21*) have reported an improved HPLC assay using the tetrapeptide Met-Ala-Ser-Trp. Since the detection of the tripeptides at 215 nm was not sensitive, several tetrapeptides Xaa-Ala-Ser-Trp, where Xaa is Met, Leu, Phe, Ile, Val, or Thr, were prepared. Hydrolysis of Met-Ala-Ser-Trp by *Ec*MetAP1, full length *Hs*MetAP1, or *Hs*MetAP1-(Δ1−66) mutant could be easily detected, while the activity of *Hs*MetAP1(Δ1−135) was undetectable (Table 2). In contrast to the absence of cleavage of the tripeptides Leu-Ala-Ser and Phe-Ala-Ser, cleavage of Leu-Ala-Ser-Trp and Phe-Ala-Ser-Trp was easily detected, although more weakly than Met-Ala-Ser-Trp. However, no cleavage of the tetrapeptides with either Ile, Val, or Thr at the N-terminus was detected, indicating that the relaxed specificity observed for the thiopeptolides did not apply to the tetrapeptide substrates.

Inhibition of Full Length and Truncated HsMetAP1s by Nonpeptidic Inhibitors. Although bacterial MetAPs share high sequence homology with mammalian type I MetAPs in the peptidase domain, the N-terminal extension is a unique feature in mammalian MetAPs that may allow inhibitors to differentiate the two groups. We have previously identified a series of nonpeptidic small molecules with inhibitory activity against *Ec*MetAP1 and *Sc*MetAP1 (*15*), and we are interested in determining whether they also inhibit full length and truncated *Hs*MetAP1s, since few, if any, *Hs*MetAP1 inhibitors have been described. We found that some of the *Ec*MetAP1 inhibitors also inhibited *Hs*MetAP1, while others did not show inhibition (Table 3). These results suggest that ideal inhibitors, which specifically inhibit bacterial MetAPs without affecting *Hs*MetAP1, can be developed for antibacterial applications. Surprisingly, the inhibitory activity was restored or partially restored for some of the inhibitors such as **5**−**7** when tested on the N-terminal-truncated mutant *Hs*MetAP1(Δ1−66). However, no direct interaction between the inhibitors and the N-terminal extension was expected.

Table 3: Inhibition of *Ec*MetAP1, *Hs*MetAP1, and *Hs*MetAP1(Δ1−66)

Compound	Structure	IC_{50} (μM) *Ec*MetAP1	*Hs*MetAP1	*Hs*MetAP1(Δ1-66)
1	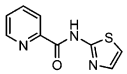	1.30 ± 0.12	10.4 ± 1.2	4.93 ± 0.68
2	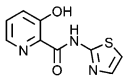	0.82 ± 0.01	8.15 ± 0.63	3.48 ± 0.35
3	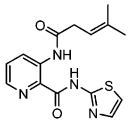	0.24 ± 0.02	14.9 ± 0.9	0.68 ± 0.03
4	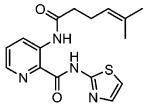	0.61 ± 0.08	7.42 ± 0.78	1.04 ± 0.08
5	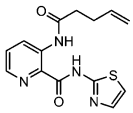	0.51 ± 0.08	>100	0.79 ± 0.08
6	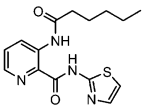	0.38 ± 0.03	86.7 ± 4.4	2.04 ± 0.29
7	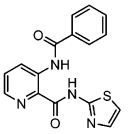	0.89 ± 0.06	>100	7.37 ± 1.06
8	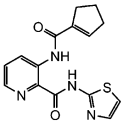	0.36 ± 0.06	>100	>100
9	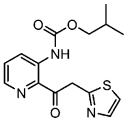	1.92 ± 0.30	>100	>100

DISCUSSION

Infectious diseases are still a serious health threat, and the rising resistance to antibiotics has created an urgency to validate novel targets for therapeutic intervention. MetAP carries out the essential function of removing the initiator Met from nascent proteins in microorganisms and is a

promising target for novel antibiotics (*11*). Common pathogenic bacteria have only a single type I MetAP. These MetAPs are homologous to *Hs*MetAP1, which along with type II MetAP (*Hs*MetAP2) carries out important physiological functions. Our successfully established *E. coli* expression system for *Hs*MetAP1 provides a useful tool for characterizing MetAP inhibitors that specifically inhibit bacterial MetAPs without affecting *Hs*MetAP1. This inhibition profile is required for effective control of infection and minimum toxicity to humans. With the recombinant *Hs*MetAP1 available, we have characterized a series of nonpeptidic *Ec*MetAP1 inhibitors and identified a few with desirable inhibition profiles that show submicromolar potencies for *Ec*MetAP1 and no activity against *Hs*MetAP1 (>100 μM).

*Hs*MetAP2 has been suggested as the in vivo target for antiangiogenic fumagillin and its analogues (*22*, *23*), while *Hs*MetAP1 has not been studied extensively. LAF389 was derived from the natural product bengamides originally isolated from marine sponges and showed good inhibition of both *Hs*MetAP1 and *Hs*MetAP2 (*24*). It causes growth inhibition in vitro at low nanomolar concentrations on all human tumor cell lines tested and significantly inhibits the growth of MDA-MB-435 human breast cancer xenografts at well-tolerated doses. The *Hs*MetAP1 inhibitors identified in this study with micromolar inhibitory activities provide tools for further investigation of the functions of *Hs*MetAP1 in physiological and pathological processes.

The functional role of the N-terminal extension in mammalian MetAPs is not yet fully understood. The extension in type I MetAPs has a zinc finger structure, while that in type II MetAPs contains polyacidic and polybasic clusters. Deletion of the extension does not significantly alter catalytic activity as in *Sc*MetAP1 (*5*) and in *Hs*MetAP2 (*18*), and it does not seem to be directly involved in enzyme catalysis. However, it has been demonstrated that deletion of this extension in *Sc*MetAP1 reduced its effectiveness in rescuing the slow growth phenotype of a *map* mutant (*5*), and the zinc finger motifs are important in the association of MetAP with the ribosome (*7*).

Deletion of the N-terminal extension was either observed during purification (*18*, and this study) or generated in vitro by trypsin digestion (*5*). This phenomenon reveals a susceptible site within the extension, and the existence of truncated eukaryotic MetAPs in vivo remains to be confirmed. Nevertheless, our truncated mutants *Hs*MetAP1(Δ1−66) and *Hs*MetAP1(Δ1−135) provide the opportunity to study the role of the extension in substrate recognition and hydrolysis and its influence on inhibition.

The N-terminal deletion of residues 1−135 from *Hs*MetAP1 was based on a sequence alignment of the peptidase domain among MetAPs and represents the longest deletion in a mammalian MetAP. Its detectable activity by the sensitive thiopeptolide assay demonstrates that peptidase domain in a mammalian MetAP is sufficient for catalysis. It had weak activity and tended to precipitate when concentration was attempted, which might be due to an improper position of the deletion or exposure of areas that were previously covered by the N-terminal extension.

MetAPs are a class of enzymes with stringent specificity toward the only natural amino acid residue Met at the N-terminus. It seems that Nle is the only other residue that can be accommodated at the Met recognition site. We have observed the hydrolysis of Nle-Ala-Ser at a comparable rate as for Met-Ala-Ser (Table 2). Bestatin-based inhibitor AHHpA-Ala-Leu-Val-Phe-OMe has an IC_{50} of 5 μM against *Ec*MetAP1 (*25*), and its (3*R*)-amino-(2*S*)-hydroxyheptanoic acid (AHHpA) moiety is a norleucine analogue. Other examples in the literature include several Met analogues in a structural study of *Ec*MetAP1 (*26*), in which trifluoromethionine, 1-amino-3-(methylmercapto)propylphosphonic acid, 1-amino-3-(methylmercapto)propylphosphinic acid, and norleucine phosphonic acid, along with Met, were used. Although both type I and type II MetAPs maintain the stringent specificity for Met, they use different sets of amino acid residues to form the S1 recognition pocket (*27*). Recently, we have made systematic mutations of the S1 site residues in *Ec*MetAP1 and *Hs*MetAP1 and identified Cys-70 in *Ec*MetAP1 and Cys-202 in *Hs*MetAP1 as crucial residues in maintaining such specificity (*28*). Interestingly, mutants *Ec*MetAP1(C70A) and *Hs*MetAP1(C202A) cleaved Phe-Ala-Ser as well as Met-Ala-Ser or Nle-Ala-Ser.

Our experiments with thiopeptolides Xaa-S-Gly-Phe have demonstrated a progressive relaxation of this specificity from the full length *Hs*MetAP1 to *Hs*MetAP1(Δ1−66) to *Hs*MetAP1(Δ1−135), suggesting a significant influence of the N-terminal extension in interacting with substrates. However, such relaxation in substrate specificity was not clear when either tripeptide or tetrapeptide substrates were used. Certainly, the thiopeptolide assay is much more sensitive than the peptide assay. It is also worth noting that the sulfur atom is significantly larger than nitrogen and a thioester linkage in thiopeptolides is longer than a amide linkage in peptides. The small but significant structural difference between thiopeptolides and peptides may account for the observed difference in the S1 specificity.

No structural information for *Hs*MetAP1 is available at this time, and the exact location of the extension is not known. According to the X-ray structure of *Hs*MetAP2 (*29*), the N-terminal extension will probably be folded on the protein surface but away from the active site. Compounds **5**−**7**, which are competitive inhibitors (*19*), inhibited the mutant *Hs*MetAP1(Δ1−66) but did not inhibit the full length *Hs*MetAP1; this inhibition profile demonstrates again the profound impact of the N-terminal extension on the enzyme active site. Further investigation is required to elucidate the mechanism by which the N-terminal extension affects the recognition and hydrolysis of substrates and the inhibition by inhibitors if it is indeed not located in the proximity of the active site.

REFERENCES

1. Bradshaw, R. A., Brickey, W. W., and Walker, K. W. (1998) N-terminal processing: the methionine aminopeptidase and N alpha-acetyl transferase families, *Trends Biochem. Sci. 23*, 263−267.
2. Tsunasawa, S., Stewart, J. W., and Sherman, F. (1985) Amino-terminal processing of mutant forms of yeast iso-1-cytochrome *c*, *J. Biol. Chem. 260*, 5382−5391.
3. Solbiati, J., Chapman-Smith, A., Miller, J. L., Miller, C. G., and Cronan, J. E. (1999) Processing of the N termini of nascent polypeptide chains requires deformylation prior to methionine removal, *J. Mol. Biol. 290*, 607−614.
4. Arfin, S. M., Kendall, R. L., Hall, L., Weaver, L. H., Stewart, A. E., Matthews, B. W., and Bradshaw, R. A. (1995) Eukaryotic

methionyl aminopeptidases: two classes of cobalt-dependent enzymes, *Proc. Natl. Acad. Sci. U.S.A. 92*, 7714−7718.
5. Zuo, S., Guo, Q., Ling, C., and Chang, Y. H. (1995) Evidence that two zinc fingers in the methionine aminopeptidase from *Saccharomyces cerevisiae* are important for normal growth, *Mol. Gen. Genet. 246*, 247−253.
6. Chang, Y. H., Teichert, U., and Smith, J. A. (1992) Molecular cloning, sequencing, deletion, and overexpression of a methionine aminopeptidase gene from *Saccharomyces cerevisiae*, *J. Biol. Chem. 267*, 8007−8011.
7. Vetro, J. A., and Chang, Y. H. (2002) Yeast methionine aminopeptidase type 1 is ribosome-associated and requires its N-terminal zinc finger domain for normal function in vivo, *J. Cell. Biol. 85*, 678−688.
8. Chang, S. Y., McGary, E. C., and Chang, S. (1989) Methionine aminopeptidase gene of *Escherichia coli* is essential for cell growth, *J. Bacteriol. 171*, 4071−4072.
9. Miller, C. G., Kukral, A. M., Miller, J. L., and Movva, N. R. (1989) PepM is an essential gene in *Salmonella typhimurium*, *J. Bacteriol. 171*, 5215−5217.
10. Li, X., and Chang, Y. H. (1995) Amino-terminal protein processing in *Saccharomyces cerevisiae* is an essential function that requires two distinct methionine aminopeptidases, *Proc. Natl. Acad. Sci. U.S.A. 92*, 12357−12361.
11. Vaughan, M. D., Sampson, P. B., and Honek, J. F. (2002) Methionine in and out of proteins: targets for drug design, *Curr. Med. Chem. 9*, 385−409.
12. Perna, N. T., Plunkett, G., Burland, V., Mau, B., Glasner, J. D., Rose, D. J., Mayhew, G. F., Evans, P. S., Gregor, J., Kirkpatrick, H. A., Posfai, G., Hackett, J., Klink, S., Boutin, A., Shao, Y., Miller, L., Grotbeck, E. J., Davis, N. W., Lim, A., Dimalanta, E. T., Potamousis, K. D., Apodaca, J., Anantharaman, T. S., Lin, J., Yen, G., Schwartz, D. C., Welch, R. A., and Blattner, F. R. (2001) Genome sequence of enterohaemorrhagic *Escherichia coli* O157: H7. *Nature 409*, 529−533.
13. Guan, K. L., and Dixon, J. E. (1991) Eukaryotic proteins expressed in *Escherichia coli*: an improved thrombin cleavage and purification procedure of fusion proteins with glutathione S-transferase, *Anal. Biochem. 192*, 262−267.
14. Zhou, Y., Guo, X. C., Yi, T., Yoshimoto, T., and Pei, D. H. (2000) Two continuous spectrophotometric assays for methionine aminopeptidase, *Anal. Biochem. 280*, 159−165.
15. Luo, Q. L., Li, J. Y., Liu, Z. Y., Chen, L. L., Li, J., Qian, Z., Shen, Q., Li, Y., Lushington, G. H., Ye, Q. Z., and Nan, F. J. (2003) Discovery and structural modification of inhibitors of methionine aminopeptidases from *Escherichia coli* and *Saccharomyces cerevisiae*, *J. Med. Chem. 46*, 2631−2640.
16. Turk, B. E., Griffith, E. C., Wolf, S., Biemann, K., Chang, Y. H., Liu, J. O. (1999) Selective inhibition of amino-terminal methionine processing by TNP-470 and ovalicin in endothelial cells, *Chem. Biol. 6*, 823−833.
17. Dummitt, B., Fei, Y., and Chang, Y. H. (2002) Functional expression of human methionine aminopeptidase type I in *Saccharomyces cerevisiae*, *Protein Pept. Lett. 9*, 295−303.
18. Yang, G., Kirkpatrick, R. B., Ho, T., Zhang, G. F., Liang, P. H., Johanson, K. O., Casper, D. J., Doyle, M. L., Marino, J. P., Thompson, S. K., Chen, W., Tew, D. G., and Meek, T. D. (2001) Steady-state kinetic characterization of substrates and metal ion specificities of the full-length and N-terminally truncated recombinant human methionine aminopeptidases (type 2), *Biochemistry 40*, 10645−10654.
19. Li, J. Y., Chen, L. L., Cui, Y. M., Luo, Q. L., Li, J., Nan, F. J., and Ye, Q. Z. (2003) Specificity for inhibitors of metal-substituted methionine aminopeptidase, *Biochem. Biophys. Res. Commun. 307*, 172−179.
20. D'souza, V. M., and Holz, R. C. (1999) The methionyl aminopeptidase from *Escherichia coli* can function as an iron(II) enzyme, *Biochemistry 38*, 11079−11085.
21. Walker, K. W., Yi, E., and Bradshaw, R. A. (1999) Yeast (*Saccharomyces cerevisiae*) methionine aminopeptidase I: rapid purification and improved activity assay, *Biotechnol. Appl. Biochem. 29*, 157−163.
22. Sin, N., Meng, L., Wang, M. Q., Wen, J. J., Bornmann, W. G., and Crews, C. W. (1997) The antiangiogenic agent fumagillin covalently binds and inhibits the methionine aminopeptidase 2, *Proc. Natl. Acad. Sci. U.S.A. 94*, 6099−6103.
23. Griffith, E. C., Su, Z., Niwayama, S., Ramsay, C. A., Chang, Y. H., and Liu, J. O. (1998) Molecular recognition of angiogenesis inhibitors fumagillin and ovalicin by methionine aminopeptidase 2, *Proc. Natl. Acad. Sci. U.S.A. 95*, 15183−15188.
24. Towbin, H., Bair, K. W., DeCaprio, J. A., Eck, M., Kim, S., Kinder, F. R., Morollo, A., Mueller, D. R., Schindler, P., Song, H. K., Oostrum, J., Versace, R. W., Voshol, J., Wood, J., Zabludoff, S., and Phillips, P. E. (2003) Proteomics based target identification: Bengamides as a new class of methionine aminopeptidase inhibitors, *J. Biol. Chem. 278*, 52964−52971.
25. Keding, S. J., Dales, N. A., Lim, S., Beauliu, D., and Rich, D. H. (1998) Synthesis of (3*R*)-amino-(2*S*)-hydroxy amino acids for inhibition of methionine aminopeptidase-1, *Synth. Commun. 28*, 4463−4470.
26. Lowther, W. T., Zhang, Y., Sampson, P. B., Honek, J. F., and Matthews, B. W. (1999) Insights into the mechanism of *Escherichia coli* methionine aminopeptidase from the structural analysis of reaction products and phosphorus-based transition-state analogues, *Biochemistry 38*, 14810−14819.
27. Lowther, W. T., and Matthews, B. W. (2000) Structure and function of the methionine aminopeptidases, *Biochim. Biophys. Acta 1477*, 157−167.
28. Li, J. Y., Cui, Y. M., Chen, L. L., Gu, M., Li, J., Nan, F. J., and Ye, Q. Z. (2004) Mutations at the S1 site of methionine aminopeptidases from *Escherichia coli* and Homosapiens reveal the residues critical for substrate specificity, *J. Biol. Chem. 279*, 21128−21134.
29. Liu, S., Widom, J., Kemp, C. W., Crews, C. M., and Clardy, J. (1998) Structure of human methionine aminopeptidase-2 complexed with fumagillin, *Science 282*, 1324−1327.

BI0360859